Electrical Power and Energy Systems 131 (2021) 106935

Contents lists available at ScienceDirect

International Journal of Electrical Power and Energy Systems

journal homepage: www.elsevier.com/locate/ijepes

An analysis of optimal power flow based formulations regarding DSO-TSO flexibility provision

Martin Bolfek [a,*], Tomislav Capuder [b]

[a] Croatia distribution system operator (HEP ODS), Croatia
[b] Faculty of Electrical Engineering and Computing, University of Zagreb, Croatia

ARTICLE INFO

Keywords:
Optimal power flow
Convex relaxation
Flexibility provision
MINLP
MISOCP

ABSTRACT

This paper establishes an optimal power flow based framework for quantifying the amount and assessing the ability of DSO to enable the provision of flexibility service to the TSO. Within this framework, a comparison of three different formulations is conducted on several real life distribution networks and IEEE test cases considering computational effort and quality of solution as metrics. By reformulating the branch flow variant of the original problem, a convex approximation approach is established and assessed with regards to exactness and suboptimality of the solution. Based on the results of smaller test cases we develop a method that is able to efficiently solve the problem for large test case instances. The results indicate significant advantages of reformulations over the classical approach on smaller test cases as well as its usefulness when solving more demanding test cases.

1. Introduction

The principles of system balancing as well as other transmission system operator (TSO) responsibilities have faced multiple challenges due to ever increasing number of intermittent generation being introduced to the grid, especially on the distribution side. It has become harder for the TSO to achieve its operational goals like balancing system generation and demand, reducing the overall system losses, maximizing social welfare and keeping the voltages within prescribed limits. The potential of the TSO-DSO interactions to increase the overall stability and efficiency of power systems has generated a substantial amount of research in this field. A comprehensive and recent literature review on this topic, can be found in [1]. In [2] a method is proposed that is able to alleviate overload in transmission network using the flexibility of a distribution network. An integral framework of leveraging distribution systems as a reactive power prosumers is developed in [3].

One cost effective way to confront system balancing issues is to exploit the positive correlation between voltage and demand by controlling the transformer on load tap changers (OLTC), capacitor banks as well as power injected into the grid by generators connected to distribution grid. Recent research, the CLASS project [4], shows that, depending on type and structure of consumption, this voltage-demand correlation can be substantial[5] and the exploitation of this correlation, when properly executed, does not significantly affect the end customers.

In this paper the focus is on determining the capability of a distribution network to adjust its active and reactive power flow at the TSO-DSO connection node by using optimization techniques, an approach that has been discussed in several papers. In [6] authors develop a linear, optimization based approach for determining distribution network's flexibility and compare their approach with nonlinear ones. Although the reduction in computational time is significant, the approach is sensitive to selection of a proper linearization point. In [7] authors develop a tractable method for determining the capability area of a network, based on a lossless linear power flow approximation. However, the method does not consider tap ratios and exhibits considerable errors when applied to networks with significant branch susceptance. Paper [8] derived a methodology for generating a DSO capability chart for TSO flexibility services provision. In order to provide the maximum response for the TSO, while at the same time satisfying operational constraints, DSO solves the optimal power flow (OPF) problem which accounts for voltage demand correlation, with optimal distribution generator's (DG) power injections, OLTC tap positions and capacitor banks shunt position as decision variables. However, the primary focus of the aforementioned paper is the OPF based concept of the TSO and DSO interaction, not the performance of the algorithm itself. The incorporation of discrete variables (OLTC, capacitor bank positions)

* Corresponding author.
E-mail addresses: martin.bolfek@hep.hr (M. Bolfek), tomislav.capuder@fer.hr (T. Capuder).

https://doi.org/10.1016/j.ijepes.2021.106935
Received 6 July 2020; Received in revised form 9 January 2021; Accepted 19 February 2021
Available online 16 May 2021

Nomenclature

Sets

N	The set of nodes in the network
N_g	The set of distributed generator nodes
B	The set of nodes with capacitor shunt banks
E	The set of *from* edges in the network
E^R	The set of *to* edges in the network
T	The set of integer transformer tap positions
sh	The set of integer shunt banks positions

Variables

p^g, q^g	Real/reactive power generation
tap	Transformer tap position
t	Transformer turns ratio in per unit
p_{sh}	Capacitor bank position
w	Voltage magnitude squared, $\|V\|^2$
l	Current magnitude squared, $\|I\|^2$
p^g_{sl}, q^g_{sl}	Active/reactive power injected at TSO-DSO connection node
$v = e + if$	Voltage in rectangular coordinates

Parameters

p^d, q^d	Real/reactive power demand
np	Real power exponential coefficient
nq	Reactive power exponential coefficient
θ^{Δ}	Voltage angle difference limit
Δt	Transformer regulation step
Δb_{sh}	Capacitor bank susceptance step
λ	Penalization parameter
δ^{ex}	Maximum cone residual
ϵ^{ex}	Maximum cone residual tolerance
ϵ^{opt}	Stopping tolerance for the difference in penalization parameters
α	Step size for the penalization parameter increase
$v^0 = e^0 + if^0$	Reference voltage magnitude
$Z = r + ix$	Line impedance
$Y = g + ib$	Line admittance
$Y^c = g^c + ib^c$	Line charging/ transformer admittance
$a_P, a_Q \in \{-1, 1\}$	Parameters used to define a search direction
ϕ	Angle between the selected search direction and real power axis
$p^{base}_{sl}, q^{base}_{sl}$	Active/reactive power at TSO-DSO connection node for the base case operating point
p_{stp}, q_{stp}	Active/reactive power at TSO-DSO connection node for desired setpoint within capability area

Other

x	a constant value
CA	Capability area problem
CA-R	Capability area problem with relaxed discrete variables
SD	Setpoint distance problem
SD-F	Feasibility setpoint distance problem
DG	Distributed generation
OLTC	On Load Tap Changer
EBF	Exact branch flow formulation
CBF	Convexified branch flow formulation

into the OPF only exacerbate performance issues. A good recent overview of different approaches that deal with discrete variables is provided in the introductory part of [9]. As authors of this paper state, most of these methods replace the discrete variables with continuous ones and use rounding to satisfy the integrality constraints. However, this method, when applied to OLTCs could easily lead to infeasibility or incur suboptimality, which is clearly demonstrated in aforementioned paper. In [10] the authors look at flexibility provision from a TSO perspective, while development of a more tractable form of OPF for large scale cases is set for future work, therefore implying that scalability of the algorithm could present an issue. In [11] the authors develop a nonlinear optimization based approach similar to [8]. While computationally efficient, the method is tested on small test cases while ignoring complexities of real distribution networks and voltage-demand correlation, all of which could result in higher computational time.

OPF is, in general, a NP hard nonconvex problem, even for a simpler case where topology of the network is radial, as shown in [12]. A substantial amount of research has been done in order to try to convexify the original OPF problem for the purpose of reaping the benefits of convex programming, such as finding the globally optimal solution, potentially increasing the tractability or providing the certificate of infeasibility for the original problem. A comprehensive and up to date survey of the topic is given in [13]. While most of the relaxations are relatively straightforward, ensuring the exactness of the relaxation remains an issue. The exactness of the relaxation for radial networks, under certain conditions, was first proved in [14]. However, as the authors of [15] show, these conditions could be very restrictive and unrealistic, so there is a reasonable chance that on realistic distribution network relaxations will be inexact making the solution physically meaningless. Furthermore, when the objective function does not steer the algorithm towards loss reduction directly or indirectly by minimizing the overall generation cost, the relaxation will always be inexact. For instance, in recent paper [16], authors formulate a multi-period OPF based problem, where the objective function is such that the convex reformulation does not necessarily lead to inexactness. However, the applicability of this approach is limited to objective being in some form of network loss reduction.

The issue of dealing with inexactness of the relaxations has been addressed by several papers in two general directions. In [17,18] the authors propose a penalization method to the semi definite programming (SDP) relaxation in order to drive the solution to AC feasibility. The major drawback of this method is the need to specify the penalization parameters. The authors in [19] propose an algorithm for calculating an appropriate objective function defined using a weighted Laplacian matrix. In [20] authors conduct a thorough analysis of several penalization methods proposed in literature by using test cases that are known to exhibit inexactness. However, the main focus of these works is the inexactness of SDP relaxation with generation cost minimization as its objective function. On the other hand, only few papers deal with the inexactness of the second order cone programming (SOCP) relaxation when applied to objectives that differ from minimizing network loss or generation cost. Authors in [21] propose a sequential convex optimization method to solve broader class of optimal power flow (OPF) problems over radial networks. In [22] authors focus on a second-order cone relaxation applied to an OPF based on a branch flow model of a radial and balanced distribution system and develop an algorithm consisting of adding an increasingly tight linear cut to the SOC relaxation in order to ensure its exactness. Authors in [23] further develop cutting planes algorithm in order to deal with inexactness of SOC relaxation in cases where the relaxation is inexact even when the objective function is to minimize network losses. However, as authors state, the algorithm is not applicable for certain objectives, such as conservative voltage reduction (CVR), an objective similar to demand response scheme presented here. In a more recent paper [24] the authors analyze, in a unified manner, several SOCP relaxations of OPF on distribution networks previously proposed in several papers. The main focus of this paper is

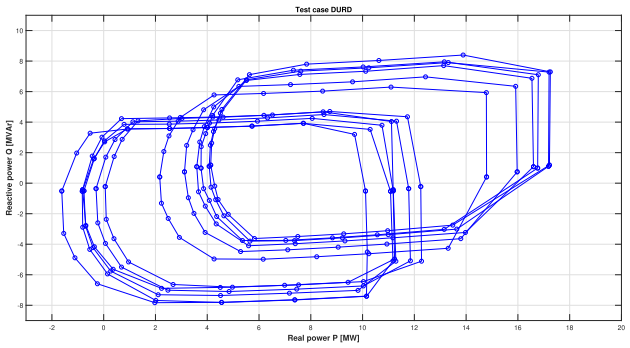

Fig. 1. An example of 12 h time evolution of distribution network capability area for **DURD** test case.

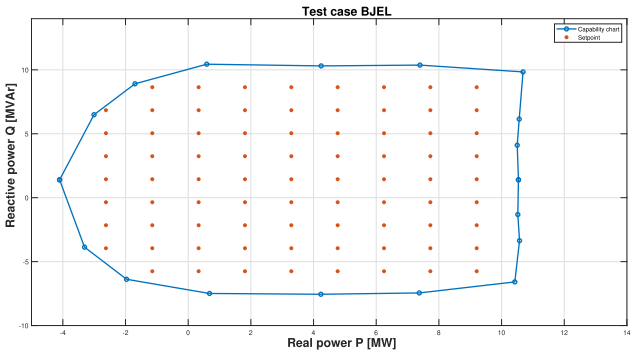

Fig. 2. An example of distribution network capability area with generated setpoints for **BJEL** test case.

the study of different approaches that are (un) able to successfully retrieve exact solutions. Authors also propose, as already proposed in [18], adding a mild penalty on current magnitudes in the objective function to achieve exactness without incurring substantial sub-optimality and claim that with this amendment SOCP relaxation can be successfully applied to a substantially wider range of objectives than the theoretically sufficient conditions suggest.

In contrast to the aforementioned papers, which discuss a specific problem in particular, here we establish a framework which is both able to determine the amount of flexibility, but also the ability of the users and assets in the distribution grid to provide the flexibility previously determined. We conduct rigorous testing on realistic test cases that encompass variable load and generation profiles, discrete variables and voltage sensitive loads in order to draw more consistent conclusions regarding the performance and solution quality. Although we consider a specific application for the methods developed, the paper suggests potentially wider applicability as we discuss convex approximation approach and its potential to provide exact solution even with objectives which inherently lead to inexactness of convex relaxations.

The main contributions of this paper are:

- We establish a two part, OPF based framework for quantifying the amount and assessing the ability of DSO to provide flexibility service to the TSO
- Within this framework, we propose a convex approximation approach and assess its performance and solution quality, with regards to standard approaches, on distribution networks which encompass discrete variables, voltage sensitive loads and detailed network modeling
- Based on the results on smaller test cases, we develop an efficient method which exploits the computational efficiency of a convex approximation approach when solving large test cases

This paper is further structured as follows. Section 2 establishes OPF based framework and discusses different formulations. Section 3 provides convex approximation approach and describes a novel algorithm developed. Section 4 discusses numerical results, in Section 5 we propose a computationally efficient method for solving large test cases, while Section 6 concludes.

2. General framework and problem formulations

2.1. Objectives

We begin by formulating, for the lack of a better term, capability area (CA) problem that provides a polygon in *P,Q* plane that quantifies distribution network's ability to change its power injection at TSO-DSO connection node. Ideally, this polygon should encompass all of real and reactive power values at the TSO-DSO connection node that can be achieved by controlling the OLTCs, capacitor shunt positions and distribution generators.

The objective function of CA problem takes the following form:

$$min \quad -\boldsymbol{a_P} p^g_{sl} \tag{1}$$

An example of 12 h evolution of the capability area is given in Fig. 1. After the capability area has been formed, we formulate a second problem, so called setpoint distance problem (SD). We first generate a number of setpoints within the capability area created and test the ability of the DSO in achieving these setpoints by formulating the objective function as minimization of the square of the Euclidean distance between the solution and the desired setpoint. In this case, the objective function takes the following form:

$$min \quad (p^g_{sl} - \boldsymbol{p}_{stp})^2 + (q^g_{sl} - \boldsymbol{q}_{stp})^2 \tag{2}$$

An example of a capability area with generated setpoints is shown in Fig. 2.

In order to ensure exactness of the further developed convex branch flow formulation, which is discussed in subsequent sections, objective functions (1) and (2) are modified in a manner where the product of square current term and inductive series component of a branch impedance is added:

$$min \quad -\boldsymbol{a_P} p^g_{sl} + \boldsymbol{\lambda} \sum_{(i,j)\in E\cup E^R} \boldsymbol{x_{ij}} l_{ij} \tag{3}$$

$$min \quad (p^g_{sl} - \boldsymbol{p}_{stp})^2 + (q^g_{sl} - \boldsymbol{q}_{stp})^2 + \boldsymbol{\lambda} \sum_{(i,j)\in E\cup E^R} \boldsymbol{x_{ij}} l_{ij} \tag{4}$$

We justify our selection of penalization term in Section 3.

2.2. Constraints in rectangular coordinates

The constraints of the OPF based model in rectangular coordinates and real numbers are given by (5)–(21). The formulation differs from the standard formulation of OPF in that Eqs. (5) and (6) encompass the voltage demand correlation, and t_{ij} and p_{shi} are now decision variables. Note here that the representation of ZIP load models (loads that consist of constant-impedance, constant-current and constant-power) in convex relaxations has been discussed in [25]. However, as authors in [4] show, although less exact, an exponential load model, which we use here, is more practical as the coefficients needed are easier to obtain on a larger scale.

$$\sum_{(i,j)\in E\cup E^R} p_{ij} = p^g_i - \boldsymbol{p^d_i}\left(\frac{e_i^2 + f_i^2}{(\boldsymbol{e_i^0})^2 + (\boldsymbol{f_i^0})^2}\right)^{\boldsymbol{np}/2} \quad \forall\ i \in N \tag{5}$$

$$\sum_{(i,j)\in E\cup E^R} q_{ij} = q^g_i - \boldsymbol{q^d_i}\left(\frac{e_i^2 + f_i^2}{(\boldsymbol{e_i^0})^2 + (\boldsymbol{f_i^0})^2}\right)^{\boldsymbol{nq}/2} + \tag{6}$$

$$p_{ij} = \left(\boldsymbol{g}_{ij}^{c} + \boldsymbol{g}_{ij}\right)\left(e_i^2 + f_i^2\right)t_{ij}^2 - t_{ij}\left[\boldsymbol{g}_{ij}\left(e_i e_j + f_i f_j\right) + \boldsymbol{b}_{ij}\left(f_i e_j - e_i f_j\right)\right] \quad (i,j) \in E \tag{7}$$

$$q_{ij} = -\left(\boldsymbol{b}_{ij}^{c} + \boldsymbol{b}_{ij}\right)\left(e_i^2 + f_i^2\right)t_{ij}^2 + t_{ij}\left[\boldsymbol{b}_{ij}\left(e_i e_j + f_i f_j\right) - \boldsymbol{g}_{ij}\left(f_i e_j - e_i f_j\right)\right] \quad (i,j) \in E \tag{8}$$

$$p_{ji} = \left(\boldsymbol{g}_{ji}^{c} + \boldsymbol{g}_{ij}\right)\left(e_i^2 + f_i^2\right) - t_{ij}\left[\boldsymbol{g}_{ij}\left(e_i e_j + f_i f_j\right) + \boldsymbol{b}_{ij}\left(f_j e_i - e_j f_i\right)\right] \quad (i,j) \in E \tag{9}$$

$$q_{ji} = -\left(\boldsymbol{b}_{ji}^{c} + \boldsymbol{b}_{ij}\right)\left(e_i^2 + f_i^2\right) + t_{ij}\left[\boldsymbol{b}_{ij}\left(e_i e_j + f_i f_j\right) - \boldsymbol{g}_{ij}\left(f_j e_i - e_j f_i\right)\right] \quad (i,j) \in E \tag{10}$$

$$\left(\boldsymbol{v}_i^{l}\right)^2 \leqslant e_i^2 + f_i^2 \leqslant \left(\boldsymbol{v}_i^{u}\right)^2 \quad \forall\, i \in N \tag{11}$$

$$p_{ij}^2 + q_{ij}^2 \leqslant \boldsymbol{s}_{ij}^2 (i,j) \in E \tag{12}$$

$$(-\boldsymbol{\theta}^{\boldsymbol{\Delta}}) \leqslant \tan^{-1}\left(\frac{f_i}{e_i}\right) - \tan^{-1}\left(\frac{f_j}{e_j}\right) \leqslant (\boldsymbol{\theta}^{\boldsymbol{\Delta}}) \quad (i,j) \in E \tag{13}$$

$$t_{ij} = tap_{ij}\boldsymbol{\Delta t_{ij}} + 1 \quad tap \in T, \quad (i,j) \in E \tag{14}$$

$$p_{shi} \in sh_i, \quad \forall i \in B \tag{15}$$

$$\boldsymbol{p}_i^{\boldsymbol{gl}} \leqslant p_i \leqslant \boldsymbol{p}_i^{\boldsymbol{gu}} \quad \forall\, i \in N_g \tag{16}$$

$$\boldsymbol{q}_i^{\boldsymbol{gl}} \leqslant q_i \leqslant \boldsymbol{q}_i^{\boldsymbol{gu}} \quad \forall\, i \in N_g \tag{17}$$

$$\left(p_i^{g}\right)^2 + \left(q_i^{g}\right)^2 \leqslant \left(\boldsymbol{s}_i^{gu}\right)^2 \quad \forall\, i \in N_g \tag{18}$$

$$q_{sl}^{g} = \boldsymbol{q}_{sl}^{base} + \boldsymbol{a_P a_Q} tan\left(\boldsymbol{\phi}\right)\left(p_{sl}^{g} - \boldsymbol{q}_{sl}^{base}\right) \tag{19}$$

$$\boldsymbol{a_P} p_{sl}^{g} \geqslant \boldsymbol{a_P q}_{sl}^{base} \tag{20}$$

$$\boldsymbol{a_Q} q_{sl}^{g} \geqslant \boldsymbol{a_Q q}_{sl}^{base} \tag{21}$$

Eqs. (5), (6) capture the active and reactive power balance where an exponential load model is used to best represent voltage dependent consumption, while (7)–(10) represent active and reactive power flows. Voltage operating constraints are given in (11), while DG real and reactive power constraints are provided in (16)–(18),. With these constraints, we model the DG capability curve similar to one of, for example, the gas turbine. However, the model could be easily extended to generators with simpler box constraints or linearized curves, usually used to model the PVs, as long as this does not change the underlying problem class. The line thermal limit constraints as well as transformer power constraints are enforced through (12). The voltage angle difference is bounded by (13). Eqs. (14) and (15) constrain the transformer tap and capacitor shunt positions. Eqs. (19)–(21), define a search direction when constructing the capability area. This is accomplished in a manner similar to [26], by alternating the values of a_P and a_Q and changing the predefined values of angle ϕ. A base case is a DSO operating point, determined, for example, in day ahead operation, for each time step.

2.3. Branch flow constraints

The constraints of the branch flow formulation are presented by (22)–(32). Two modifications of the original formulation from [27] are done in order to include the voltage-demand dependency in (23), (24) and to simplify the terms in (25), (26) by setting the imaginary part of tap position $t_{ij}^{I} = 0$.

$$\left(\boldsymbol{v}_i^{l}\right)^2 \leqslant w_i \leqslant \left(\boldsymbol{v}_i^{u}\right)^2 \ \forall i \in N \tag{22}$$

$$p_i^{g} - \boldsymbol{p}_i^{d}\left(\frac{w_i}{\boldsymbol{w_0}}\right)^{\boldsymbol{np}/2} = \sum_{(i,j)\in E\cup E^R} p_{ij} \ \forall i \in N \tag{23}$$

$$q_i^{g} - \boldsymbol{q}_i^{d}\left(\frac{w_i}{\boldsymbol{w_0}}\right)^{\boldsymbol{nq}/2} + p_{shi}\boldsymbol{\Delta b_{shi}} w_i = \sum_{(i,j)\in E\cup E^R} q_{ij} \ \forall i \in N \tag{24}$$

$$\left(-\boldsymbol{x}_{ij}\boldsymbol{g}_{ij}^{c} - \boldsymbol{r}_{ij}\boldsymbol{b}_{ij}^{c}\right)w_i t_{ij}^2 + \boldsymbol{x}_{ij}p_{ij} - \boldsymbol{r}_{ij}q_{ij} \geqslant \tan(-\boldsymbol{\theta}^{\boldsymbol{\Delta}})\left(\left(1 + \boldsymbol{r}_{ij}\boldsymbol{g}_{ij}^{c} + \boldsymbol{x}_{ij}\boldsymbol{b}_{ij}^{c}\right)w_i t_{ij}^2 - \boldsymbol{r}_{ij}p_{ij} - \boldsymbol{x}_{ij}q_{ij}\right) \tag{25}$$

$$\left(-\boldsymbol{x}_{ij}\boldsymbol{g}_{ij}^{c} - \boldsymbol{r}_{ij}\boldsymbol{b}_{ij}^{c}\right)w_i t_{ij}^2 + \boldsymbol{x}_{ij}p_{ij} - \boldsymbol{r}_{ij}q_{ij} \leqslant \tan(\boldsymbol{\theta}^{\boldsymbol{\Delta}})\left(\left(1 + \boldsymbol{r}_{ij}\boldsymbol{g}_{ij}^{c} + \boldsymbol{x}_{ij}\boldsymbol{b}_{ij}^{c}\right)w_i t_{ij}^2 - \boldsymbol{r}_{ij}p_{ij} - \boldsymbol{x}_{ij}q_{ij}\right) \tag{26}$$

$$p_{ij} + p_{ji} = \boldsymbol{r}_{ij}l_{ij}^{'} + \boldsymbol{g}_{ij}^{c}w_i t_{ij}^2 + \boldsymbol{g}_{ji}^{c}w_j \ \ (i,j) \in E \tag{27}$$

$$q_{ij} + q_{ji} = \boldsymbol{x}_{ij}l_{ij}^{'} - \boldsymbol{b}_{ij}^{c}w_i t_{ij}^2 - \boldsymbol{b}_{ji}^{c}w_j \ \ (i,j) \in E \tag{28}$$

$$\left(1 + 2\left(\boldsymbol{r}_{ij}\boldsymbol{g}_{ij}^{c} - \boldsymbol{x}_{ij}\boldsymbol{b}_{ij}^{c}\right)\right)w_i t_{ij}^2 - w_j = 2\left(\boldsymbol{r}_{ij}p_{ij} + \boldsymbol{x}_{ij}q_{ij}\right) - \left(\boldsymbol{r}_{ij}^2 + \boldsymbol{x}_{ij}^2\right)l_{ij}^{'} \ \ (i,j) \in E \tag{29}$$

$$p_{ij}^2 + q_{ij}^2 = w_i t_{ij}^2 l_{ij} \ \ (i,j) \in E \tag{30}$$

$$p_{ij}^2 + q_{ij}^2 \leqslant \boldsymbol{s}_{ij}^2 (i,j) \in E \tag{31}$$

$$\left(p_i^{g}\right)^2 + \left(q_i^{g}\right)^2 \leqslant \left(\boldsymbol{s}_i^{gu}\right)^2 \quad \forall\, i \in N_g \tag{32}$$

where

$$l_{ij}^{'} = l_{ij} - 2\left(\boldsymbol{g}_{ij}^{c}p_{ij} - \boldsymbol{b}_{ij}^{c}q_{ij}\right) + \left(\boldsymbol{y}_{ij}^{c}\right)^2 w_i t_{ij}^2$$

2.4. Convex relaxation of the branch flow constraints

Due to equality in (30), the alterations in (23), (24) and the introduction of integer variables that represent transformer tap and capacitor bank positions, the problem at hand is still a mixed integer nonconvex problem. In this section we deal with the introduced nonlinearities in order to establish the convex model.

2.4.1. Voltage-demand dependency

We use the a first order Taylor approximation in order to linearize the terms in (23) and (24). The term $\left(\frac{w_i}{\boldsymbol{w_0}}\right)^{\boldsymbol{np}/2}$ is expanded, for simplicity, around voltage of $\boldsymbol{w}_0 = 1$ p.u. leading to:

$$\left(\frac{w_i}{\boldsymbol{w_0}}\right)^{\boldsymbol{np}/2} \approx 1 + \frac{\boldsymbol{np}}{2}(w_i - 1) \tag{33}$$

2.4.2. Transformer turns ratio and capacitor banks shunt position

When transformer tap changers are decision variables, a nonlinear term $w_i t_{ij}^2$ makes the formulation non convex. In order to address this we consider an approach from [28] which develops the exact linear relaxation of the aforementioned term. The main idea is to introduce a new variable w^{tr} for each primary side of OLTC equipped transformer, for which the following holds:

$$w^{tr} = \sum_{i=1}^{|T|} a_i \boldsymbol{b}_i w \tag{34}$$

where a_i is a binary variable such that

$$\sum_{i=1}^{|T|} a_i = 1 \tag{35}$$

Table 1
Formulation description.

Form. name	Capability area (CA)		Setpoint distance (SD)	
	Obj.	Constraints	Obj.	Constraints
Rect.	(1)	(5)–(21)	(2)	(5)–(18)
CBF	(3)	(16)–(29), (31)–(41)	(4)	(16)–(18), (22)–(29), (31)–(41)
EBF	(1)	(16)–(40)	(2)	(16)–(18),(22)–(40)

and b is a constant value calculated for each tap position:

$$\boldsymbol{b} = \boldsymbol{t}^2 = (\boldsymbol{tap}\Delta\boldsymbol{t} + 1)^2 \quad \forall\, tap \in T \tag{36}$$

However, a bilinear term in (34) still exist. This term is transformed to linear constraint by using McCormick inequalities:

$$w^{tr} \geqslant a_i \boldsymbol{b}_i \boldsymbol{w}^{\boldsymbol{l}} \tag{37}$$

$$w^{tr} \leqslant a_i \boldsymbol{b}_i \boldsymbol{w}^{\boldsymbol{u}} \tag{38}$$

$$w^{tr} \geqslant \boldsymbol{b}_i (w + \boldsymbol{w}^{\boldsymbol{u}} a_i - \boldsymbol{w}^{\boldsymbol{u}}) \tag{39}$$

$$w^{tr} \leqslant \boldsymbol{b}_i (w + \boldsymbol{w}^{\boldsymbol{l}} a_i - \boldsymbol{w}^{\boldsymbol{l}}) \tag{40}$$

The convexification of the product $p_{shi}w_i$ regarding the capacitor banks is done in the same manner but is here omitted for brevity.

2.4.3. Introducing conic constraint

With the introduction of a new variable w^{tr} from (34) a term in (30) is relaxed with an inequality that takes the form of a rotated SOC constraint:

$$p_{ij}^2 + q_{ij}^2 \leqslant w_i^{tr} l_{ij} \quad (i,j) \in E \tag{41}$$

Finally, we summarize the formulations for two problems of interest in Table 1.

The first formulation is the classical OPF based formulation in rectangular coordinates belonging to a class of mixed integer nonlinear programs (MINLP). A similar and well known formulation with polar coordinates is not examined as our initial testing showed considerably poorer performance when compared to rectangular formulation, which is in line with observations in [29] where authors state that, although conceptually similar, polar and rectangular formulation can exhibit substantial difference in tractability.

The second formulation is convex reformulation of the Extended Branch Flow variant of the problem from [27], here referred to as Convexified Branch Flow (CBF). This formulation belongs to a class of mixed integer second order cone programs (MISOCP).

The third (re) formulation, here referred to as Exact Branch Flow (EBF), is based on CBF with the exception of not relaxing the nonlinear constraint in (30). It serves as a reference for analysing the quality of solutions of the previous two formulations.

3. Convex approximation

In order to ensure exactness of a convex relaxation, we use a penalization approach where we add a penalization term that minimizes current magnitude to the objective function in (3) and (4). However, adding a penalization term could influence the objective function in a manner that favors loss reduction over maximization of real power exchange between DSO and TSO. In other words, relaxation could be made exact, but suboptimal at the same time.

Unlike usual approaches where only current magnitude squared is penalized, here we decide to penalize the product of current magnitude squared and inductive series component of a branch/transformer impedance. As our analysis shows, this allows for a wider range of penalization parameter values for which the CBF is exact and still does not incur substantial suboptimality as illustrated on **jag** test case in Fig. 3.

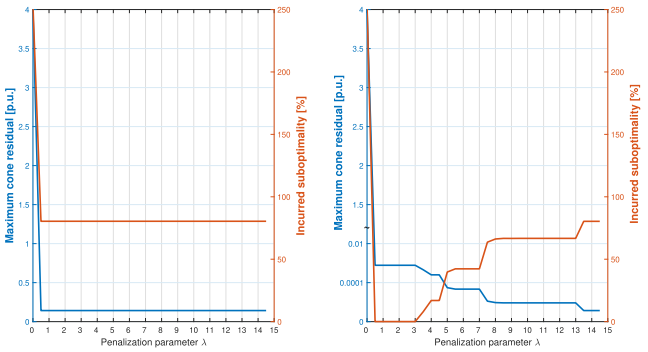

Fig. 3. An example of changes in incurred suboptimality and resulting maximum cone residual with changes in penalization parameter for **jag** test case. The left graph shows the changes when only the $\sum l$ is penalized in the objective, while the right graph shows the changes when $\sum xl$ is penalized.

The right graph of the figure also shows that as the value of penalization parameter is increased, three distinct sets of solutions are produced by an optimization algorithm. First set of solutions for which the relaxation is inexact, and therefore physically meaningless. This is reflected in high value of residual in (41). Second set of solutions, for which relaxation is exact and penalization parameter is not set high enough to influence the objective, and the third set for which relaxation is again exact, but influences the result in favor of loss reduction which is reflected in substantial suboptimality incurred. Having these observations in mind, a simple bisection algorithm that finds the appropriate penalization parameters is proposed and further explained. The solution procedure is given by Algorithm 1. Note that the developed approximation approach is based on the existence of the set of solutions which yields exactness and does not incur suboptimality. Although we do not provide evidence that such set is non-empty, our testing suggests the procedure provided could be applied to a wide range of distribution networks while its theoretical guarantees are left for future work.

3.1. Bisection algorithm

Let δ^{ex}, defined by (42), denote the maximum cone residual that is evaluated in post processing in order to determine the exactness of the relaxation.

$$\delta^{ex} = max(|p_{ij}^2 + q_{ij}^2 - \frac{w_i}{t_{ij}^2} l_{ij}|) \quad (i,j) \in E \tag{42}$$

Let α denote step size and ϵ^{ex} and ϵ^{opt} denote the convergence criteria for the exactness of the relaxation and difference between values of λ^{ex} and λ^{rel}. After setting the appropriate convergence criteria and step size, we compute the CBF with λ initially set to 0. If the SOC constraint in CBF is not met with equality up to a predefined precision, we update variable λ^{rel}, corresponding to penalization parameter that provided non exact solution, and run another instance of CBF with (3) as an objective function with increased value of penalization parameter λ.

If the penalization parameter that provides the exact solution is found, the corresponding λ^{ex} is updated and the algorithm proceeds to bisection part, which ensures that the penalization parameter that does not incur substantial suboptimality is found.

Algorithm 1. Determining penalization parameter

Input: $\epsilon^{ex}, \epsilon^{opt}, \alpha, \lambda = 0$
repeat
Run CBF
Compute δ^{ex}

(*continued on next page*)

Table 2
Test cases description.

Test case	Nodes	Lines	Trafo	Voltage lvl.	OLTCs	Cap.
case kpc	18	8	9	35 kV	9	5
case durd	9	4	4	35 kV	4	3
IEEE 33bus	33	34	1	12.66 kV	1	-
IEEE 69bus	69	72	1	12.66 kV	1	-
case bjel	20	9	11	35 kV	8	3
case jag	60	22	37	20 kV	1	4
case sok	165	119	60	20 kV	3	5
case kop1	466	456	9	20 kV	9	8

Table 3
Generators active/reactive power limits [MW/MVAr]

Test case	DGs	P_{min}	P_{max}	Q_{min}	Q_{max}
case kpc	2	0	1	−0.7	0.7
case durd	1	0	10	−5	5
IEEE 33bus	6	0.1	1	−0.2	0.1
IEEE 69bus	2	0.1	1	−0.2	0.1
case bjel	3	0	1/2/10	−0.5/-1/-6.2	0.5/1/6.2
case jag	1	0	1	−0.5	0.5
case sok	3	0	1.5	−0.75	0.75
case kop1	6	0	1	−0.75	0.75

Table 4
Number of variables and constraints.

	CBF		Rectangular	
Test case	# Variables	# Constraints	# Variables	# Constraints
case kpc	599	1076	89	151
case durd	282	503	44	74
IEEE 33bus	358	465	145	263
IEEE 69bus	674	861	281	551
case bjel	553	970	96	168
case jag	627	849	246	600
case sok	1672	2234	673	1578
case kop1	4675	6070	1892	3735

(*continued*)

if $\delta^{ex} > \epsilon^{ex}$ **then**
  $\lambda^{rel} \leftarrow \lambda$
  $\lambda \leftarrow \lambda + \alpha$
else
  $\lambda^{ex} \leftarrow \lambda$
end if
until $\delta^{ex} > \epsilon^{ex}$
if $\lambda^{ex} \neq 0$ **then**
repeat
  $\lambda \leftarrow \frac{\lambda^{rel} + \lambda^{ex}}{2}$
  Run CBF
  Compute δ^{ex}
  if $\delta^{ex} > \epsilon^{ex}$ **then**
    $\lambda^{rel} \leftarrow \lambda$
  else
    $\lambda^{ex} \leftarrow \lambda$
  end if
until $\lambda^{ex} - \lambda^{rel} > \epsilon^{opt}$
end if

4. Numerical results and discussion

4.1. Test cases and setup

The numerical results were performed on several real distribution networks in Croatia as well as two modified test cases (33bus and 69bus) from [30,31] respectfully. The test cases are of different voltage level which implies varying degree of complexity. The total number of nodes, transformers, capacitor banks and generators are shown in Table 2 and Table 3 for each test case provided. The total number of variables and constraints for different formulations of a CA problem are shown in Table 4 for each test case. Note that CA and SD problem differ only in a small number of variables and constraints overall.

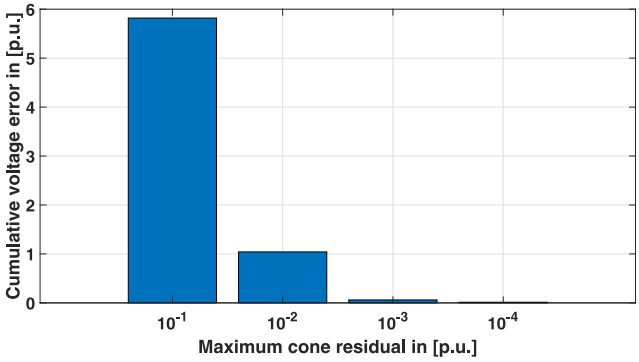

Fig. 4. Cumulative voltage error change for smaller test cases with varying degree of allowable cone residual.

The power lines are represented as a standard π model. The transformers are modeled in the same manner, except that here, the shunt admittance is comprised of iron losses (g^c) and magnetizing susceptance (b^c), calculated from transformer nameplate. They are equipped with OLTCs, with ±10 steps and 1.5%voltage change per step in all cases. Each capacitor bank is assumed to have six steps in all test cases.

The real and reactive power consumption data are based on 24 h time interval measurements for real distribution networks while for IEEE test cases, the consumption data provided serves as a baseline on top of which data for all 24 h is generated based on typical load profile for a distribution network in Croatia. The data is provided for one day, in one hour time interval. The capability curves are estimated separately, so there are no time coupling constraints.

We assume that the network is observable up to a required degree, that the coefficients of the exponential model are determined in advance for each substation. The voltage constraints are all set to ±10% of the nominal voltage. The effectiveness of demand increase or reduction greatly depends on proper determination of voltage upper and lower bounds and should be carefully predetermined, as in [32]. Exponential coefficients *np* and *nq* are set to 1.1 and 3 respectively. In order to provide a fair result comparison, the voltage demand correlation is only approximately modeled as in (33) in all formulations. An exact voltage-demand correlation in CBF cannot be directly introduced to the formulation, however, given that these are only approximately determined, this presents only a minor issue. The distribution networks used in this paper are operated radially. The CBF formulation used here is not guaranteed to provide physically meaningful solutions when dealing with mesh topology, even when penalization approach is applied. However, more tight SOC relaxations do exist like the one in [33] which is effective for meshed transmission networks.

Regarding the setup of the Algorithm 1, we set $\epsilon^{ex} = 10^{-3}$, $\epsilon^{opt} = 0.1$ and $\alpha = 0.5$. Note here that the changes in daily load profiles result in only minor changes in penalization parameters, therefore, once the appropriate parameters are found, the number of subsequent iterations in the next time step, needed for determining the parameter, is significantly reduced. This is achieved by setting the initial λ values to values already determined from the previous time step. The justification for the selected maximum cone residual tolerance (parameter ϵ^{ex}) is based on the results of an analysis as shown in Fig. 4. We first calculated the DG set point values, OLTC and capacitor bank positions with CBF formulation variant of a CA problem with different cone residual tolerances and then used the aforementioned decision variables as inputs for simple

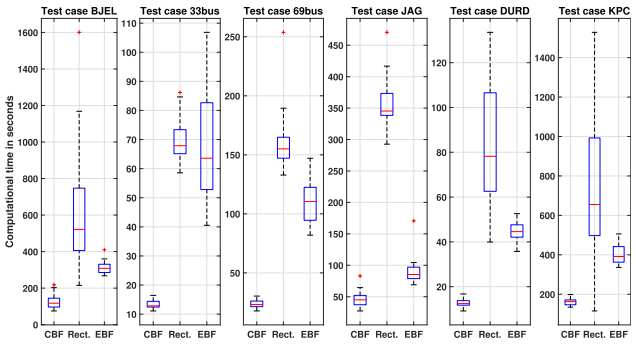

Fig. 5. Distribution of computational effort for creation of one hour time step capability area.

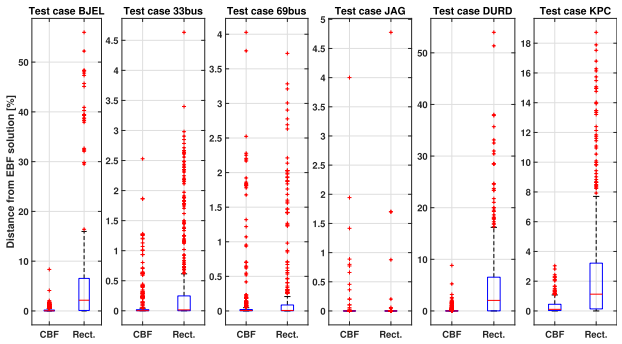

Fig. 6. Relative Euclidean distance of solutions provided by rectangular formulation and CBF compared to EBF.

power flow calculation. We then calculated the sum of all the differences between the node voltages provided by the power flow calculation and their respective upper or lower voltage bound if the resulting node voltage violates that bound. As shown in Fig. 4, this cumulative voltage error is almost negligible for a selected tolerance of 10^{-3}.

For CA problem the ϕ, a_P and a_Q parameters are set in order to generate 20 points of the capability area around a base point which is generated as a result of a variant of OPF that minimizes the overall network losses. In total, 480 runs are conducted per test case. For SD problem, between 60 and 70 setpoints have been generated, for each time step, depending on the size of capability curve, which implies around 1440 runs per test case have been conducted.

Experiments are carried out on PC with Intel i5-3470 CPU and 6 GB memory. Optimization problems are coded in MATLAB with YALMIP toolbox [34]. The CBF fomulation is solved using CPLEX v.12.9. [35], rectangular formulation is solved using KNITRO v.12.1. [36] and EBF is solved using SCIP v5.01 solver[37]. Maximum time of 600 s for calculating SD or CA problem for each point of a capability area is set for all solvers. Computational times reported for CBF are calculated by adding times for all iterations of Algorithm 1 needed to obtain adequate solution. Finally, a note on solver setup. In order to more accurately compare the effort of the solvers used, the available options for KNITRO solver were modified, to the best of authors knowledge, to match the default ones in CPLEX. Furthermore, on test cases with a large number of integer variables, KNITRO solver is not able to close the gap between a relaxed solution and current one with tolerances already set to match CPLEX default ones. In these cases, a tolerance for aforementioned relative gap is set to 1% for both solvers. This modification makes KNITRO computational effort comparable to CPLEX without incurring substantial suboptimality when considering real life application. Given the difference in solver tolerance settings, for cases with a large number of integer variables, the results presented do not necessarily reflect problems difficulty. With these adjustments in solver settings we try to ensure there is minimum bias in solutions provided, regardless of the solver selected.

4.2. Computational effort – capability area problem

The distribution of the computational times needed for creating capability area for one time step, per test case, for all three formulations is presented in Fig. 5. by using standard MATLAB box-and-whiskers plot where the central mark indicates the median, and the bottom and top edges of the box indicate the 25th and 75th percentiles, respectively. The whiskers extend to the most extreme data points not considered outliers, and the outliers are plotted individually using the '+' symbol.

The method proposed performs well on smaller test cases even with relatively high number of discrete decision variables. However, already on a medium sized test case (case **sok**) both EBF and rectangular formulation fail to provide results within set time limitation in most instances. The CBF formulation is able to provide results within 1200 s. However, on a large test case (case **kop1**) all of the methods are unable to find optimal result within the time limitation. On smaller test cases, the CBF formulation, in terms of tractability, outperforms EBF and rectangular formulations overall, on some test cases by the factor of 9. Because of the way the Algorithm 1 is designed, most of the calculation time for the CBF formulation is spent in the first time step in order to find an appropriate penalization parameter for the specific test case. Once found, there is only a small difference in penalization parameter for different time steps, usually only reflecting the change in load for every segment. If the load does not change drastically from adjacent time steps, Algorithm 1 requires only 2–3 iterations in order to converge. The CBF is also the most consistent one of the three, which is reflected in small difference between minimum and maximum values and relatively small number of outliers. This is contrary to rectangular formulation which performs well on average, but can have problems with certain time steps, hitting the specified time limit. These differences cannot be observed when dealing with test cases that do not provide time varying load data, which could lead to false interpretation of the results. These results also expose the shortcomings of testing on relatively simple test cases derived from literature as rectangular formulation performs well on these cases, but shows poorer performance on real life and more demanding test cases. The scalability issues motivate a development of a method that is able to provide meaningful results in a realistic time frame and is presented in Section 5.

Somewhat surprising is the performance of EBF formulation, which is on most of the smaller cases comparable or better then the rectangular one and is outperforming the rectangular formulation up to factor of 4 on JAG test case. A global MINLP solver is able to certify most of the results as the globally optimal ones, while still providing feasible solutions in cases where a global optimal solution is not reached. The use of of-the-shelf global optimization solvers for OPF problems, to the best of our knowledge, has not been studied extensively. However, as discussed in [38–40], global optimization solvers could benefit greatly from reformulations, strengthening variable bounds and adding valid inequalities to the original problem which is in line with results presented

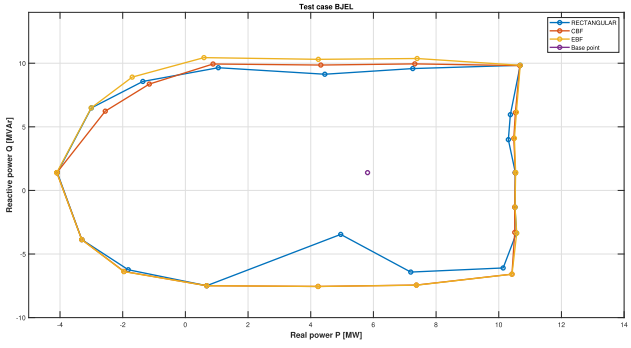

Fig. 7. An example of capability area with noticeable differences between different formulations.

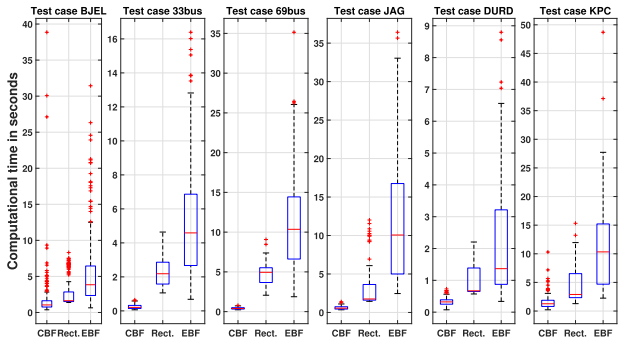

Fig. 8. Distribution of computational times for minimizing the distance to a specific setpoint.

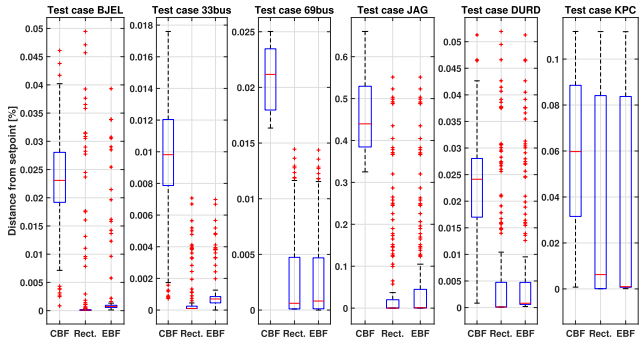

Fig. 9. Distribution of relative distance of solutions provided by each formulation to the desired setpoint value.

here. Still, the CBF approach outperforms EBF by up to a factor of 9 in **33bus** test case.

4.3. Solution quality – capability area problem

The results representing the quality of solutions provided by CBF and rectangular formulation are presented in Fig. 6. The results are reported only for those test cases where all the formulations are able to provide solutions within the set time limit. Each plot summarizes the distribution of 480 values for each of the two formulations. The quality of solution is expressed in percentage, measured as a relative Euclidean distance of a real and reactive power exchange in TSO-DSO connection node produced by CBF and rectangular formulation compared to optimal solution produced by EBF. The greater the distance, the more conservative the area produced by specific formulation is, example of which is shown in Fig. 7. Both CBF and rectangular formulation provide negligible suboptimality on test cases with smaller number of OLTCs. Rectangular formulation exhibits poorer results already on DURD test case with the maximum distance of around 17%. The maximum distance provided by rectangular formulation on KPC test case is 8%, but with a notable number of outliers. On BJEL test case the suboptimality reaches 17% for rectangular formulation. However, the median values are satisfactory overall, reaching just 4% for rectangular formulation on BJEL test case. The CBF formulation performs almost the same as EBF with maximum outlier of only 9% on BJEL test case.

4.4. Computational effort – setpoint distance problem

The distribution of computational time needed for each formulation to minimize the distance to each specific setpoint is provided by Fig. 8. CBF outperforms the EBF and rectangular one, usually requiring only two iterations in finding the appropriate penalization parameter that satisfies the cone residual threshold. Contrary to previous problem analyzed, in this case the computational times do not exhibit substantial difference making all of them applicable even when considering real time applications.

4.5. Solution quality – setpoint distance problem

The distribution of relative setpoint distance for each formulation is provided by Fig. 9. All of the setpoints generated are achieved within a fraction of percent in all test cases. Because of the approximation approach needed, the CBF provides the greatest distances, but these are negligible in any case. An important note here is that all of the formulations were able to achieve all the desired setpoints which were generated within the least conservative capability curves, the ones produced by EBF in previous problem. This shows that although CBF and rectangular formulations could not find solutions through capability area problem, they were able to provide solutions through setpoint distance problems for setpoints that were outside their respective capability areas.

5. Method for solving large test cases

As numerical test show, on smaller test cases, even when the number of discrete variables is substantial, all tested formulations produce results within reasonable time frame. However, rectangular and EBF formulation are, in most instances, unable even to provide a result already on medium size test case and the same can be observed for CBF on a large test case. In this section we present a method that is able to solve the CA problem on large instances based on observations made in previous sections. As it can be seen, the computational effort for SD problem is substantially lower then for CA problem on all test cases. We therefore propose a two step method to solve the original CA problem where we first relax the discrete variables and solve the original CA problem more efficiently and then use the obtained solution as a setpoint around which, within some reasonable tolerance, we find a feasible solution.

Let us define new variants of CA and SD problem. We denote CA-R a variant of CA problem as defined in Table 1 but here we relax binary variables a_i from (34) and (35) which can now take any value from 0 to 1. We denote SD-F a variant of SD problem as defined by Table 1 but without an objective function and with the following additional constraint:

$$(p_{sl}^{g} - \boldsymbol{p}_{stp})^2 + (q_{sl}^{g} - \boldsymbol{q}_{stp})^2 \leqslant \epsilon^{dist} \tag{43}$$

where ϵ^{dist} denotes a tolerance, agreed upon between TSO and DSO, with regards to the desired values of real and reactive power at interconnection node.

The method developed is illustrated by Algorithm 2. First, we solve a CBF variant of CA-R problem. In order to ensure the exactness of the CA-R problem, we have to employ an Algorithm 1 in the same manner as when dealing with the original CA problem. The outputs of CA-R problem are values of real and reactive power at the TSO-DSO connection node for predefined number of outermost points of a capability area. In the second part, we use the outputs from the previous computation which now enter a SD-F problem as parameters $\boldsymbol{p}_{stp}$ and $\boldsymbol{q}_{stp}$.

Algorithm 2. Solving large test cases

Input: $\epsilon^{ex}, \epsilon^{opt}, \alpha, \lambda = 0$
Run CBF variant of CA-R problem with Algorithm 1
Output: p_{sl}^{g}, q_{sl}^{g}
$\boldsymbol{p}_{stp} \leftarrow p_{sl}^{g}$
$\boldsymbol{q}_{stp} \leftarrow q_{sl}^{g}$
Input: $\epsilon^{dist}, \boldsymbol{p}_{stp}, \boldsymbol{q}_{stp}$
Run Rectangular variant of SD-F problem

The increase in computational efficiency is achieved by two major changes with regards to the original CA and SD problems. Since we have

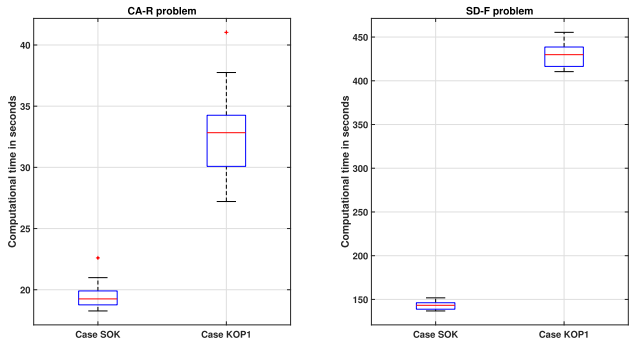

Fig. 10. Distribution of computational effort of CA-R and SD-F problem for creation of one hour time steps capability area for medium and large size test cases.

relaxed all binary variables, CA-R is now a SOCP problem which is less computational demanding than the original MISOCP problem. In SD-F, the variables regarding OLTC and capacitor bank position remain discrete, but here we only solve a feasibility problem, meaning we only want to obtain one feasible solution where the constraint (43) ensures obtaining a satisfactory solution. In this case, the solver used can be set to stop at first feasible solution which results in significant reduction of computation time. We apply the proposed method to a medium size (case **sok**) and a large size test case (**kop1**). The computational efficiency of the proposed method is shown by Fig. 10. As expected, the CBF formulation on a relaxed CA problem is efficient and is able to generate the one hour capability curve in less then 20 s on **sok** test case and less then 40 s on **kop1** test case. For a feasibility problem, MINLP solver requires less then 150 s on a medium size test case and less then 450 s for a large sized one. Overall, the proposed method is able to generate a one hour capability curve in less then 500 s overall for a demanding, large size test case with a substantial number of discrete variables.

6. Conclusion and future work

This paper formulates two OPF based problems - the problem of determining the capability area for distribution network flexibility provision at one hand, and the ability to set the available controlling devices, in order to achieve desired setpoint within the aforementioned curve. The two problems encompass voltage dependent loads, OLTC and capacitor bank positions which makes them computationally demanding. This motivates the development of the proposed convex approximation approach as well as a more detailed study of a known branch flow reformulation. Within the established framework, the comparison of three different formulations is conducted with computational effort and quality of solution as metrics. Based on results on smaller to medium sized networks, we develop and asses a method that can effectively solve large test case instances.

As our results indicate, when applied to the problem at hand, the classical optimization approach would require a development of a specially tailored algorithms that exploit the specific problem structure or an in depth knowledge of a certain solver in order to be applicable in realistic scenarios. With the classical approach, the use of of-the-shelf solvers on large instances, with a substantial number of discrete variables is rather optimistic. The CBF formulation, combined with a novel algorithm, outperforms other formulations, in some cases by several orders of magnitude, while still providing solutions with relatively small suboptimality.

Finally, the convex approximation approach developed shows it is able to provide feasible solutions, usually with negligible gaps, when compared to globally optimal ones, even when applied to objectives for which a similar convex *relaxation* would inevitably lead to infeasible results. This paper shows, along several other ones, that approximation approaches significantly broaden the applicability of convex reformulation of the original OPF, far more than theoretically suggested.

CRediT authorship contribution statement

Martin Bolfek: Conceptualization, Methodology, Writing - original draft, Visualization, Investigation. **Tomislav Capuder:** Software, Validation, Resources, Supervision, Writing - review & editing.

Declaration of Competing Interest

The authors declare that they have no known competing financial interests or personal relationships that could have appeared to influence the work reported in this paper.

Acknowledgment

The research leading to these results has received funding from the European Union's Horizon 2020 research and innovation programme under Grant Agreement No 864579 (project FLEXIGRID). The sole responsibility for the content of this document lies with the authors. It does not necessarily reflect the opinion of the Innovation and Networks Executive Agency (INEA) or the European Commission (EC). INEA or the EC are not responsible for any use that may be made of the information contained therein. The work is supported by Croatian Science Foundation (HRZZ) and Croatian Distribution System Operator (HEP ODS) through project IMAGINE - Innovative Modelling and Laboratory Tested Solutions for Next Generation of Distribution Networks (PAR-2018).

Appendix A. Supplementary material

Supplementary data associated with this article can be found, in the online version, at https://doi.org/10.1016/j.ijepes.2021.106935.

References

[1] Gonzalez DM, Myrzik J, Rehtanz C. The smart power cell concept: Mastering TSO-DSO interactions for the secure and efficient operation of future power systems. IET Gener Transm Distrib 2020;14(13):2407–18.
[2] Jin X, Mu Y, Jia H, Wu Q, Jiang T, Wang M, Yu X, Lu Y. Alleviation of overloads in transmission network: A multi-level framework using the capability from active distribution network. Int J Electrical Power Energy Syst 2019; 112: 232–51. Available: http://www.sciencedirect.com/science/article/pii/S0142061519305137.
[3] Zhou Y, Li Z, Yang M. A framework of utilizing distribution power systems as reactive power prosumers for transmission power systems. Int J Electric Power Energy Syst 2020; 121:106139. Available: http://www.sciencedirect.com/science/article/pii/S0142061520304543.
[4] Ballanti A, Ochoa LN, Bailey K, Cox S. Unlocking new sources of flexibility: CLASS: the world's largest voltage-led load-management project. IEEE Power Energ Mag 2017;15(3):52–63.
[5] Ballanti A, Ochoa LF. Initial assessment of voltage-led demand response from UK residential loads. In: 2015 IEEE power and energy society innovative smart grid technologies conference, ISGT 2015; 2015.
[6] Contreras DA, Rudion K. Improved assessment of the flexibility range of distribution grids using linear optimization. In: 20th Power Systems Computation Conference, PSCC 2018; 2018. p. 1–7.
[7] Fortenbacher P, Demiray T. Reduced and aggregated distribution grid representations approximated by polyhedral sets. Int J Electric Power Energy Syst 2020; 117: 105668. Available: http://www.sciencedirect.com/science/article/pii/S0142061519309159.
[8] Capitanescu F. TSO–DSO interaction: Active distribution network power chart for TSO ancillary services provision. Electric Power Syst Res 2018;163:226–30.
[9] Shukla SR, Paudyal S, Almassalkhi MR. Efficient distribution system optimal power flow with discrete control of load tap changers. IEEE Trans Power Syst 2019;34(4):2970–9.
[10] Capitanescu F. AC OPF-Based methodology for exploiting flexibility provision at TSO/DSO interface via oltc-controlled demand reduction. In: 20th Power Systems Computation Conference, PSCC 2018. IEEE; 2018. p. 1–6.
[11] Silva J, Sumaili J, Bessa RJ, Seca L, Matos M, Miranda V. The challenges of estimating the impact of distributed energy resources flexibility on the TSO/DSO boundary node operating points. Comput Oper Res 2018; 96: 294–304. Available: http://www.sciencedirect.com/science/article/pii/S0305054817301417.
[12] Lehmann K, Grastien A, Van Hentenryck P. AC-feasibility on tree networks is NP-hard. IEEE Trans Power Syst 2016;31(1):798–801.

[13] Molzahn DK, Hiskens IA. A survey of relaxations and approximations of the power flow equations. Surv Relax Approx Power Flow Equ 2019;4(1–2):1–221.
[14] Lavaei J, Low SH. Zero duality gap in optimal power flow problem. IEEE Trans Power Syst 2012;27(1):92–107.
[15] Christakou K, Tomozei DC, Le Boudec JY, Paolone M. AC OPF in radial distribution networks – Part I: On the limits of the branch flow convexification and the alternating direction method of multipliers. Electric Power Syst Res 2017;143:438–50.
[16] Yang W, Chen L, Deng Z, Xu X, Zhou C. A multi-period scheduling strategy for ADN considering the reactive power adjustment ability of DES. Int J Electrical Power Energy Syst 2020;121:106095.
[17] Madani R, Sojoudi S, Lavaei J. Convex relaxation for optimal power flow problem: Mesh networks. IEEE Trans Power Syst 2015;30(1):199–211.
[18] Madani R, Ashraphijuo M, Lavaei J. Promises of conic relaxation for contingency-constrained optimal power flow problem. In: 2014 52nd annual Allerton conference on communication, control, and computing, Allerton 2014; 2014, vol. 31, no. 2, pp. 1064–1071.
[19] Molzahn DK, Josz C, Hiskens IA, Panciatici P. A Laplacian-based approach for finding near globally optimal solutions to OPF problems. IEEE Trans Power Syst 2017;32(1):305–15.
[20] Venzke A, Chatzivasileiadis S, Molzahn DK. Inexact convex relaxations for AC optimal power flow: Towards AC feasibility. Electric Power Syst Res 2020;187. p. arXiv:1902.04815.
[21] Wei W, Wang J, Li N, Mei S. Optimal power flow of radial networks and its variations: a sequential convex optimization approach. IEEE Trans Smart Grid 2017;8(6):2974–87.
[22] Abdelouadoud SY, Girard R, Neirac FP, Guiot T. Optimal power flow of a distribution system based on increasingly tight cutting planes added to a second order cone relaxation. Int J Electrical Power Energy Syst 2015;69:9–17.
[23] Gao H, Liu J, Wang L, Liu Y. Cutting planes based relaxed optimal power flow in active distribution systems. Electric Power Syst Res 2017;143:272–80.
[24] Bobo L, Venzke A, Chatzivasileiadis S. Second-order cone relaxations of the optimal power flow for active distribution grids: Comparison of methods. Int J Electrical Power Energy Syst 2021; 127: 106625. Available: https://linkinghub.elsevier.com/retrieve/pii/S0142061520341703.
[25] Shen Z, Wei Z, Sun G, Chen S. Representing ZIP loads in convex relaxations of optimal power flow problems. Int J Electrical Power Energy Syst 2019; 110: 372–85. Available: http://www.sciencedirect.com/science/article/pii/S0142061518330151.
[26] Kalantar-Neyestanaki M, Sossan F, Bozorg M, Cherkaoui R. Characterizing the reserve provision capability area of active distribution networks: a linear robust optimization method. IEEE Trans Smart Grid 2020;11(3):2464–75.
[27] Coffrin C, Hijazi HL, Van Hentenryck P. DistFlow Extensions for AC Transmission Systems, Arxiv.org; 2015. Available: http://arxiv.org/abs/1506.04773.
[28] Zhao T, Zhang J. Representing tap-changer transformers in conic relaxation optimal power flows. Int J Eng Sci Invent ISSN 2016; 5 (6): 2319–6734. Available: www.ijesi.org.
[29] Torres GL, Quintana VH. AN interior-point method for nonlinear optimal power flow using voltage rectangular coordinates. IEEE Trans Power Syst 1998;13(4):1211–8.
[30] Baran ME, Wu FF. Network reconfiguration in distribution systems for loss reduction and load balancing. IEEE Trans Power Delivery 1989;4(2):1401–7.
[31] Parasher R. Load flow analysis of radial distribution network using linear data structure; 2014. arXiv e-prints, p. arXiv:1403.4702. Available: http://arxiv.org/abs/1403.4702.
[32] Ballanti A, Ochoa LF. Voltage-led load management in whole distribution networks. IEEE Trans Power Syst 2018;33(2):1544–54.
[33] Coffrin C, Hijazi HL, Van Hentenryck P. The QC relaxation: a theoretical and computational study on optimal power flow. IEEE Trans Power Syst 2016; 31 (4): 3008–18. Available: http://arxiv.org/abs/1502.07847.
[34] Löfberg J. YALMIP: A toolbox for modeling and optimization in MATLAB. In: Proceedings of the IEEE international symposium on computer-aided control system design; 2004. p. 284–9.
[35] IBM. Ibm Ilog Cplex; 2009. p. 1. Available: www.ibm.com.
[36] Byrd RH, Nocedal J, Waltz RA. Knitro: An integrated package for nonlinear optimization. In: Di Pillo G, Roma M., editors, Large-scale nonlinear optimization. Boston, MA: Springer, US; 2006. p. 35–59.
[37] Gamrath G, Anderson D, Bestuzheva K, Chen W-K, Eifler L, Gasse M, et al. "The SCIP Optimization Suite 7.0," Optimization Online, Tech. Rep. 05; 2020.
[38] Coffrin C, Hijazi HL, Van Hentenryck P. Strengthening convex relaxations with bound tightening for power network optimization. In: Pesant G, editor, Lecture Notes in Computer Science (including subseries Lecture Notes in Artificial Intelligence and Lecture Notes in Bioinformatics), vol. 9255. Cham: Springer International Publishing; 2015. p. 39–57.
[39] Kocuk B. Global optimization methods for optimal power flow and transmission switching problems in electric power systems; 2016. p. 204. Available: https://smartech.gatech.edu/handle/1853/55633.
[40] Liu J, Laird CD, Scott JK, Watson JP, Castillo A. Global solution strategies for the network-constrained unit commitment problem with AC transmission constraints. IEEE Trans Power Syst 2019;34(2):1139–50.